

## Catalytic Role of Gold in Gold-Based Catalysts: A Density Functional Theory Study on the CO Oxidation on Gold

Zhi-Pan Liu and P. Hu\*

Contribution from the School of Chemistry, The Queen's University of Belfast, Belfast, BT9 5AG, UK

Ali Alavi

Department of Chemistry, University of Cambridge, CB2 1EW, United Kingdom

Received April 24, 2002

**Abstract:** Gold-based catalysts have been of intense interests in recent years, being regarded as a new generation of catalysts due to their unusually high catalytic performance. For example, CO oxidation on Au/TiO<sub>2</sub> has been found to occur at a temperature as low as 200 K. Despite extensive studies in the field, the microscopic mechanism of CO oxidation on Au-based catalysts remains controversial. Aiming to provide insight into the catalytic roles of Au, we have performed extensive density functional theory calculations for the elementary steps in CO oxidation on Au surfaces. O atom adsorption, CO adsorption, O<sub>2</sub> dissociation, and CO oxidation on a series of Au surfaces, including flat surfaces, defects and small clusters, have been investigated in detail. Many transition states involved are located, and the lowest energy pathways are determined. We find the following: (i) the most stable site for O atom on Au is the bridge site of step edge, not a kink site; (ii) O<sub>2</sub> dissociation on Au (O<sub>2</sub>→2O<sub>ad</sub>) is hindered by high barriers with the lowest barrier being 0.93 eV on a step edge; (iii) CO can react with atomic O with a substantially lower barrier, 0.25 eV, on Au steps where CO can adsorb; (iv) CO can react with molecular O<sub>2</sub> on Au steps with a low barrier of 0.46 eV, which features an unsymmetrical four-center intermediate state (O–O–CO); and (v) O<sub>2</sub> can adsorb on the interface of Au/TiO<sub>2</sub> with a reasonable chemisorption energy. On the basis of our calculations, we suggest that (i) O<sub>2</sub> dissociation on Au surfaces including particles cannot occur at low temperatures; (ii) CO oxidation on Au/inactive-materials occurs on Au steps via a two-step mechanism: CO+O<sub>2</sub>→CO<sub>2</sub>+O, and CO+O→CO<sub>2</sub>; and (iii) CO oxidation on Au/active-materials also follows the two-step mechanism with reactions occurring at the interface.

### 1. Introduction

Gold had long been regarded as being catalytically far less active than many transition metals.<sup>1–4</sup> However, since the pioneering work of Haruta, it has been found that gold can exhibit surprisingly high catalytic reactivity when it is highly dispersed on reducible metal oxides (e.g., TiO<sub>2</sub>).<sup>1,2,4</sup> Au/oxides catalysts have now become one of the hottest systems in catalysis, being widely applied to many important processes, such as CO oxidation, partial oxidation of hydrocarbons, and hydrogenation of unsaturated hydrocarbons.<sup>1,5–9</sup> Among these processes, CO oxidation on Au-based catalysts is of particular interest.<sup>1,4,8</sup> Technologically, it is extensively used in exhaust emission control and sensors. Scientifically, it is widely utilized

as a model system to understand the high reactivity of Au/oxides because of the simplicity of CO oxidation. Although a large number of experiments for CO oxidation on Au-based catalysts<sup>1–31</sup> have been reported, the origin of the catalytic role that gold plays still remains unclear. Many basic issues, such

\* To whom correspondence should be addressed. E-mail: P.Hu@qub.ac.uk.

(1) Haruta, M.; Date, M. *Appl. Catal. A. Gen.* **2001**, *222*, 427.  
 (2) Haruta, M. *Catal. Today* **1997**, *36*, 153.  
 (3) Hammer, B.; Norskov, J. K. *Nature* **1995**, *376*, 238.  
 (4) Valden, M.; Lai, X.; Goodman, D. W. *Science* **1998**, *281*, 1637.  
 (5) Hayashi, T.; Tanaka, K.; Haruta, M. *J. Catal.* **1998**, *178*, 556.  
 (6) Jia, J.; Haraki, K.; Kondo, J. N.; Domen, K.; Tamaru, K. *J. Phys. Chem. B* **2000**, *104*, 11 153.  
 (7) Bianchi, C.; Porta, F.; Prati, L.; Rossi, M. *Top. Catal.* **2000**, *13*, 231.  
 (8) Bond, G. C.; Thompson, D. T. *Catal. Rev. Sci. Eng.* **1999**, *41*, 319.  
 (9) Cosandey, F.; Madey, T. E. *Surf. Rev. Lett.* **2001**, *8*, 73.

(10) Ruggiero, C.; Hollins, P. *Chem. Soc. Faraday Trans.* **1996**, *92*, 4829.  
 (11) Canning, N. D. S.; Outka, D. A.; Madix, R. J. *Surf. Sci.* **1984**, *141*, 240.  
 (12) Paker, D. H. and Koel, B. E. *J. Vac. Sci. Technol. A* **1990**, *8* (3), 2585.  
 (13) Bondzie, V. A.; Parker, S. C.; Campbell, C. T. *J. Vac. Sci. Technol. A* **1999**, *17*, 1717.  
 (14) Iizuka, Y.; Tode, T.; Takao, T.; Yatsu, K.; Takeuchi, T.; Tsubota, S. et al., *J. Catal.* **1999**, *187*, 50.  
 (15) Dekkers, M. A. P.; Lippits, M. J.; Nieuwenhuys, B. E. *Catal. Lett.* **1998**, *56*, 195.  
 (16) Bocuzzi, F.; Chiorino, A.; Manzoli, M.; Lu, P.; Akita, T.; Ichikawa, S.; Haruta, M. *J. Catal.* **2001**, *202*, 256.  
 (17) Grunwaldt, J.-D.; Baiker, A. *J. Phys. Chem.* **1999**, *103*, 1002.  
 (18) Liu, H.; Kozlov, A. I.; Kozlova, A. P.; Shido, T.; Asakura, K.; Iwasawa, Y. *J. Catal.* **1999**, *185*, 252.  
 (19) Tripathi, A. K.; Kamble, V. S.; Gupta, N. M. *J. Catal.* **1999**, *187*, 332.  
 (20) Valden, M.; Pak, S.; Lai, X.; Goodman, D. W. *Catal. Lett.* **1998**, *56*, 7.  
 (21) Grunwaldt, J. D.; Kiener, C.; Wogerbauer, C.; Baiker, A. *J. Catal.* **1999**, *186*, 458.  
 (22) Mavrikakis, M.; Stoltze, P.; Norskov, J. K. *Catal. Lett.* **2000**, *64*, 101.  
 (23) Schubert, M. M.; Hackenberg, S.; van Veen, A. C.; Muhler, M.; Plzak, V.; Behm, R. J. *J. Catal.* **2001**, *197*, 113.  
 (24) Haruta, M.; Tsubota, S.; Kobayashi, T.; Kageyama, H.; Genet, M. J.; Delmon, B. *J. Catal.* **1993**, *144*, 175.  
 (25) Bollinger, M. A.; Vannice, M. A. *Appl. Catal. B* **1996**, *8*, 417.  
 (26) Tsubota, S.; Nakamura, K.; Tanaka, K.; Haruta, M. *Catal. Lett.* **1998**, *56*, 131.

as whether O<sub>2</sub> dissociates on Au particles, are highly controversial.<sup>1,2,23</sup> Aiming to provide insight into the remarkable catalytic activity of Au-based catalysts, in this work we have used CO oxidation on Au as a model system to understand the Au-based catalysts. We have calculated, for the first time, many important elementary steps in CO oxidation on a range of Au surfaces using density functional theory (DFT). We will show where and how (i) O<sub>2</sub> is activated; and (ii) CO is oxidized on Au surfaces.

Experimentally, it has been found that CO oxidation can take place on supported Au catalysts at low temperature and the efficiency depends critically on the method of catalyst preparation.<sup>1–4</sup> Au single crystals, for their simplicity, have been extensively studied concerning CO oxidation. A general consensus is the following: (i) CO can reversibly adsorb on Au at low temperatures (up to 150 K).<sup>11</sup> (ii) Oxygen dissociative adsorption at temperatures below 673 K is strongly hindered by a high barrier.<sup>12</sup> (iii) CO oxidation takes place readily only when oxygen is provided in atomic form.<sup>12,13</sup> Interestingly, Iizuka et al.<sup>14</sup> recently found that Au powders (diameter 76 nm) with preoxidative treatment at 423 K, are able to convert CO to CO<sub>2</sub> at the room temperature. The reason for this enhanced activity was yet unclear, and was speculated to relate either to the small size effect of Au powders or to the preoxidative treatment.

For supported Au catalysts, it is generally agreed that CO can adsorb on dispersed gold particles, as evidenced by IR spectra.<sup>15–20</sup> However, the mechanism of oxygen adsorption and activation, which is essential for CO oxidation on supported Au catalysts, are much in debate. Two mechanisms have been proposed and they differ from each other on where and how molecular O<sub>2</sub> are activated.

The first mechanism suggests that highly dispersed Au particles are already catalytically active.<sup>1,14,21,22</sup> It was proposed in this mechanism that on the active sites, (i) O<sub>2</sub> can adsorb; and (ii) O<sub>2</sub> either directly dissociates or interacts with CO forming a four-center surface complex, a labile precursor state for CO oxidation. The role of supported metal oxides is limited to the stabilization of the small Au particles. Evidence that supports this mechanism is that CO oxidation can occur on Au particles supported on irreducible oxides, such as SiO<sub>2</sub> and Al<sub>2</sub>O<sub>3</sub> (inert materials).<sup>1,23,29a,29b</sup> Indeed, the Au particle size effect on the efficiency of CO oxidation on Au-based catalysts has been observed by many groups. Small Au particles appear far more active than large ones. Recently, Goodman and co-workers found that there is a critical thickness of gold layers, which gives a maximum in catalytic activity of gold nanoparticles deposited on a single-crystal surface of TiO<sub>2</sub>.<sup>4</sup>

The second mechanism suggests that the adsorption and the activation of O<sub>2</sub> are largely related to the supporting materials:<sup>23–28</sup> They occur either dominantly on the support or at the

metal/support interface. For example, Haruta et al. proposed that a carbonate-like intermediate (–CO<sub>3</sub>) may exist at the Au/support interface, which is a precursor state for CO<sub>2</sub> formation.<sup>2,24</sup> Liu et al. suggested that O<sub>2</sub> first adsorbs on defects sites of metal oxides, and then dissociate into O atoms to react with a coming CO.<sup>27</sup> On the basis of their isotopic tracing experiment,<sup>23</sup> Schubert et al. preferred a mechanism that O<sub>2</sub> directly dissociates into O atoms at the Au/support interface, which then reacts with CO.

Compared to the large volume of experimental work, theoretical studies for CO oxidation on Au-based catalysts are rather rare. Mavrikakis et al.<sup>22</sup> studied in detail the adsorption behavior of O atom and CO adsorption on flat Au(111) and stepped Au(211) using DFT. They showed that there is little variation in the chemical activity of Au(111) with the slab thickness, whereas steps were found to bond more strongly with the adsorbates than the (111) terraces. Recently, O<sub>2</sub> adsorption on small Au clusters have been studied by several groups (e.g., Okumura et al.,<sup>30a</sup> Mills et al.<sup>30b</sup> and Salisbury et al.<sup>30c</sup>). They suggested that negatively charged Au atoms are possible active sites for O<sub>2</sub> adsorption. To date, no theoretical work on the reaction pathways and energetics of CO oxidation on Au-based catalysts have been reported.

To clarify the controversies regarding where and how O<sub>2</sub> is activated on Au, we have used DFT calculations as “computer experiments” to explore possible answers for the following questions: (i) Can O<sub>2</sub> directly dissociate on Au surfaces? (ii) How does CO react with atomic O on Au and what is the reaction barrier? (iii) Can CO directly react with molecular O<sub>2</sub>? To map out low-energy pathways for these reactions, various Au surfaces, including flat surfaces, defects, and clusters, have been used. Transition states (TSs) have been located, and reaction barriers determined. Because these reactions, i.e., O<sub>2</sub> dissociation, reactions involving O atom and O<sub>2</sub> molecule, are prototypical reactions for many other oxidative systems, the results presented here are of general interest.

This paper is organized as follows. The calculation methods are mentioned in detail in section 2. The calculated results, including O atom adsorption, O<sub>2</sub> dissociation, CO adsorption, and CO oxidation with O atom and molecular O<sub>2</sub> were shown in section 3. Some important analyses and discussions on our results were also presented. In the last part of section 3 (3.4), we will discuss the possible mechanisms for CO oxidation on Au-based catalysts. Finally, the conclusions are summarized.

## 2. Calculation Details

Density functional theory with a GGA-PBE<sup>32a</sup> functional, as implemented in the program CASTEP,<sup>33a</sup> was used for all the total energy calculations. The electronic wave functions were expanded in a plane wave basis set and the ionic cores were described by ultrasoft pseudopotentials.<sup>33b</sup> Perdew et al. have demonstrated that the GGA-PBE functional showed somewhat improved energetics compared to the GGA-PW91 functional.<sup>32</sup> In this work, the O<sub>2</sub> molecule bonding energy in the gas phase was calculated to be 5.52 eV (PBE), which agrees better with

- (27) Liu, H.; Kozlov, A. I.; Kozlova, A. P.; Shido, T.; Iwasawa, Y. *Phys. Chem. Chem. Phys.* **1999**, *1*, 2851.  
(28) Kozlov, A. I.; Kozlova, A. P.; Liu, H.; Iwasawa, Y. *Appl. Catal. A Gen.* **1999**, *182*, 9.  
(29) (a) Grisel, R. J. H.; Nieuwenhuys, B. E. *J. Catal.* **2001**, *199*, 48.; (b) Sanchez, A.; Abbet, S.; Heiz, U.; Schneider, W.-D.; Hakkinen, H.; Barnett, R. N.; Landman, U. *J. Phys. Chem. A* **1999**, *103*, 9573.  
(30) (a) Okumura, M.; Kitagawa, Y.; Haruta, M.; Yamaguchi, K.; *Chem. Phys. Lett.* **2001**, *346*, 163. (b) Mills, G.; Gordon, M. S.; Metiu, H. *Chem. Phys. Lett.* **2002**, *359*, 493. (c) Salisbury, B. E.; Wallace, W. T.; Whetten, R. L. *Chem. Phys.* **2000**, *262*, 131.  
(31) Date, M.; Haruta, M. *J. Catal.* **2001**, *201*, 221.

- (32) (a) Perdew, J. P.; Burke, K.; Ernzerhof, M. *Phys. Rev. B* **1996**, *77*, 3865.; (b) Perdew, J. P.; Chevary, J. A.; Vosko, S. H.; Jackson, K. A.; Pederson, M. R.; Singh, D. J.; Fiolhais, C. *Phys. Rev. B* **1992**, *46*, 6671.  
(33) (a) Payne, M. C.; Teter, M. P.; Allan, D. C.; Arias, T. A.; Joannopoulos, J. D. *Rev. Mod. Phys.* **1992**, *64*, 1045. (b) Vanderbilt, D. *Phys. Rev. B* **1990**, *41*, 7892.

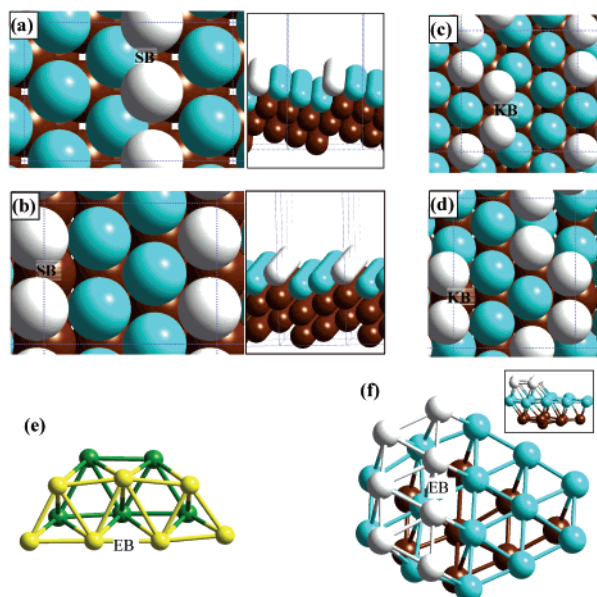


**Figure 1.** Illustration of the geometrical structures of calculated Au surfaces including Au clusters. (a) The top view (left) and side view (right) of the Au(221) surface; the dotted line shows the  $(1 \times 2)$  unit cell of Au(211). The step-edge Au atoms are white balls. SB labels the step-edge bridge site. (b) The same as (a), except that it is a Au(211) surface. (c) The top view of Au kink-I, which is constructed by taking one step-edge Au atom from the  $(1 \times 3)$  unit cell of Au(221). KB labels the kink-edge bridge site. (d) The same as (c), except that it is a Au kink-II which is derived from the Au(211). (e) An optimized 12-atom Au cluster. The white balls and dark balls are the top layer and the second layer Au atoms, respectively. EB labels the step-edge bridge site. (f) The top view and side view (insert) of an optimized 29-atom Au cluster. EB labels the step-edge bridge site. The structure is constructed to mimic a step on the Au cluster. The three-layer Au atoms are labeled by white balls, light blue balls and brown balls, respectively.

experimental value ( $\sim 5.12$  eV) than that (5.67 eV) calculated by the GGA-PW91 functional.<sup>32b</sup> For Au, an 11-electron relativistic ultrasoft pseudopotential was used. The Au dimer ( $\text{Au}_2$ ) bonding energy has been tested and it was found that the calculated value (2.23 eV) is in good agreement with experimental data (2.29 eV). The vacuum region between slabs was  $10 \text{ \AA}$  and a cutoff energy of 340 eV was used. Monkhorst–Pack  $\mathbf{k}$ -point sampling with  $0.07 \text{ \AA}^{-1}$  spacing is utilized for all the calculations (for example, for a  $p(2 \times 2)$  Au(111) slab,  $3 \times 3 \times 1$   $\mathbf{k}$ -point sampling is used). Systems which may possess net spin have been checked using spin-polarized DFT.

The Au(111) surface is modeled by a  $p(2 \times 2)$  unit cell. Au-steps are modeled by Au(211) and Au(221) using a  $(1 \times 2)$ ,  $(1 \times 3)$ , or  $(1 \times 4)$  unit cells, where necessary. Figure 1a and b illustrates the  $(1 \times 2)$  unit cells of Au(211) and Au(221), respectively. The steps of Au(211) and Au(221) are very similar except that the steps in Au(211) is of  $\{100\}$  structure, whereas it is of  $\{111\}$  structure in Au(221). The Au-kinks are modeled by removing one Au atom from the step in a  $(1 \times 3)$  unit cell of Au(221) (named kink-I, Figure 1c) or Au(211) (named kink-II, Figure 1d). In the slab-calculations, the surfaces are modeled with 3 layers (or effectively 3 layers in the cases of steps, kinks, see the side view of Figure 1a and b). The top layer is relaxed, whereas the other two layers are fixed at their bulk-truncated structure.

We have also done calculations on two different Au clusters, a 12-atom cluster (Figure 1e) and a 29-atom cluster<sup>34</sup> (Figure 1f), to model Au particles. It should be borne in mind that the

Au clusters might be different from real supported Au particles. The two clusters were constructed to be as closely packed as possible, and to mimic particular structures of Au particles. The 12-atom cluster mimics the common edges of Au particles. The 29-atom cluster that has a  $\{100\}$  step mimics Au particles with monatomic-steps and most of faces exposed are closely packed (see Figure 1f) with some (100) face. In the cluster-calculations, the clusters were placed in the center of the periodic cell with the vacuum region being  $8\sim 10 \text{ \AA}$ , large enough to avoid the lateral interaction. All the degrees of freedoms of atoms in the periodical cells were allowed to relax. Transition states (TSs) of the catalytic reactions were searched by constraining the distance between the reactants and relaxing all the other degrees of freedom, the so-called constrained minimization technique.<sup>35–40,42,43</sup> The TS was identified when (i) the force on the atoms vanish and (ii) the energy is a maximum along the reaction coordinate, but a minimum with respect to all the remaining degrees of freedom. Our previous work has demonstrated that the above DFT setup affords a good accuracy, especially for the calculation of reaction barriers in heterogeneous catalysis.<sup>35–40</sup>

### 3. Results and Discussions

**3.1 O Atom Adsorption and  $\text{O}_2$  Dissociation.** As we mentioned in the Introduction, whether  $\text{O}_2$  molecules dissociate into atomic O in CO oxidation on Au-based catalysts is uncertain. Although there is evidence that  $\text{O}_2$  cannot directly dissociate on Au single crystals at the room temperature, it is not clear that this is true on small Au particles. It has been speculated that small Au particles that possess a large number of defects may be active enough to dissociate  $\text{O}_2$ .<sup>14,21,22</sup> The remarkable enhancement effect of steps on dissociating diatomic molecules, e.g., NO and  $\text{N}_2$  on transition metal surfaces has already been found in recent experiments and theoretical calculations.<sup>45–51</sup> For instance, the reaction barrier of  $\text{N}_2$  dissociation on Ru(0001) is more than 1 eV, whereas it is reduced to be about 0.4 eV on the Ru-steps.<sup>46</sup> In the following subsection, we first show our calculated results for the O atom

- (34) The electronic structure of very small Au clusters (containing 2–10 Au atoms) have been studied by several groups using DFT: (a) Hakkinen, H.; Landman, U. *Phys. Rev. B* **2000**, *62*, 4. (b) Gronbeck, H.; Andreoni, W. *Chem. Phys.* **2000**, *262*, 1.
- (35) Liu, Z.-P.; Hu, P. *J. Am. Chem. Soc.* **2001**, *123*, 12 596.
- (36) Liu, Z.-P.; Hu, P. *J. Chem. Phys.* **2001**, *114*, 8244.
- (37) Liu, Z.-P.; Hu, P.; Alavi, A. *J. Chem. Phys.* **2001**, *114*, 5956.
- (38) Liu, Z.-P.; Hu, P. *J. Chem. Phys.* **2001**, *115*, 4977.
- (39) Zhang, C. J.; Hu, P. *J. Am. Chem. Soc.* **2001**, *123*, 1166; Zhang, C. J.; Hu, P. *J. Am. Chem. Soc.* **2000**, *122*, 2134.
- (40) Zhang, C. J.; Hu, P.; Alavi, A. *J. Am. Chem. Soc.* **1999**, *121*, 7931.
- (41) (a) Bleakey, K.; Hu, P. *J. Am. Chem. Soc.* **1999**, *121*, 7644; (b) Zhang, C. J.; Hu, P.; Lee, M.-H. *Surf. Sci.* **1999**, *432*, 305; (c) Lynch, M.; Hu, P. *Surf. Sci.* **2000**, 458, 1.
- (42) Michaelides, A.; Hu, P. *J. Am. Chem. Soc.* **2001**, *123*, 4235; Michaelides, A.; Hu, P. *J. Am. Chem. Soc.* **2000**, *122*, 9866.
- (43) Sachs, C.; Hildebrand, M.; Volkening, S.; Wintterlin, J.; Ertl, G. *Science* **2001**, *293*, 1635.
- (44) Alavi, A.; Hu, P.; Deutsch, Th.; Silvestrelli, P. L.; Hutter J. *Phys. Rev. Lett.* **1998**, *80*, 3650.
- (45) Zambelli, T.; Wintterlin, J.; Trost, J.; Ertl, G. *Science* **1996**, *273*, 1688.
- (46) Dahl, S. Logadottir, A. Egeberg, R. C. Larsen, J. H. Chorkendorff. *I. Phys. Rev. Lett.* **1999**, *83*, 1814.
- (47) Dahl, S.; Tornqvist, E.; Chorkendorff. *I. J. Catal.* **2000**, *192*, 381.
- (48) Liu, Z.-P.; Hu, P. Unpublished results.
- (49) (a) News, D. M. *Phys. Rev.* **1969**, *178*, 1123; (b) Hammer, B.; Norskov, J. K. *Adv. Catal.* **2000**, *45*, 6671; (c) Hoffmann, R. *Rev. Mod. Phys.* **1988**, *60*, 601; (d) Hammer, B.; Norskov, J. K.; *Surf. Sci.* **1995**, *343*, 211.
- (50) (a) Shustorovich, E.; Baetzold, R. C.; Muettterties, E. L.; *J. Phys. Chem.* **1983**, *87*, 1100; (b) Hu, P.; King, D. A.; Lee, M.-H.; Payne, M. C. *Chem. Phys. Lett.* **1995**, *246*, 73.
- (51) Hammer, B. *Phys. Rev. Lett.* **1999**, *83*, 3681.

**Table 1.** O Atom Adsorption Energy on the Most Stable Adsorption Site ( $E_{\text{ad}}(\text{O})$ ) of Different Gold Surfaces<sup>a</sup>

	$E_{\text{ad}}(\text{O})$ (eV)	site	CN
Au(111)	2.47 <sup>(1/4 ML)</sup> 2.78 <sup>(1/9 ML)</sup>	fcc hollow	9
Au(221)	2.91	SB	7
Au(211)	3.09	SB	7
Au kink-I	2.72	KB	6
Au kink-II	2.71	KB	6
12-atom	2.58	EB	6
29-atom	2.63	EB	7
Au-adatom	1.74	top	1

<sup>a</sup> The coordination number (CN) of Au that bonds with O atom is also listed. The labelings for the adsorption site for Au(211), Au(221), Au kink-I, Au kink-II, 12-atom cluster, and 29-atom cluster are showed in Figure 1. The Au-adatom is modeled by putting a Au atom on the fcc hollow site in a  $p(2 \times 2)$  unit cell of Au(111), and the O adsorbs on the top of this adatom.

adsorption on various Au surfaces including defects and then the  $\text{O}_2$  direct dissociation on these surfaces. We will also rationalize these results in conjunction with the current theoretical models and the experimental facts.

**3.1.1 O Atom Adsorption.** As a starting point, we calculated O atom chemisorption energies on a series of different Au surfaces, namely the flat Au(111), Au(211) (the surface with  $\{100\}$  steps), Au(221) (surface with  $\{111\}$  steps), kinked Au surfaces (kink-I and kink-II, see calculation methods in section 2) and small clusters. All the calculated O adsorption energies ( $E_{\text{ad}}(\text{O})$ ) on the corresponding most stable adsorption site of these surfaces are listed in Table 1 (see Figure 1 for the labeling of the adsorption site). In Table 1, we also labeled the coordination number (CN) of the Au atoms, on which the adsorbed O atom sits. The CN of a Au atom is defined by the number of its nearest neighboring Au atoms (for example, the CN of Au atom in the bulk Au metal is 12, and it is 9 for the (111) surface atoms). The results are described as follows:

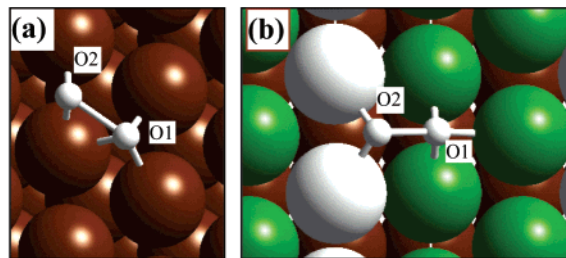
On the flat Au(111) (the CN is 9), the O atom prefers the fcc 3-fold hollow site. The  $E_{\text{ad}}(\text{O})$  is 2.47 eV at the 1/4 monolayer (ML) and the average O–Au distance,  $d_{\text{O–Au}}$ , is 2.163 Å. The  $E_{\text{ad}}(\text{O})$  increases to 2.78 eV at the 1/9 ML and the  $d_{\text{O–Au}}$  remains almost unchanged. The  $E_{\text{ad}}$  is similar to a half of an O–O bond (the O–O bond is calculated to be 5.50 eV; the experimental value: 5.2 eV). This implies that the  $\text{O}_2$  dissociative adsorption on the flat Au(111), if it occurs at all, is not strongly exothermic. The values of  $E_{\text{ad}}$  is consistent with the previous work by Mavrikakis et al.<sup>22</sup>

On both Au(221) and Au(211), the most stable site for O atom is the bridge site of monatomic step edge (the CN is 7, labeled SB in Figure 1a and b). The  $E_{\text{ad}}(\text{O})$  increases by several tenth eV compared to the flat Au(111), i.e., 2.91 and 3.09 eV on Au(221) and Au(211), respectively. The  $d_{\text{O–Au}}$  is slightly shortened compared to that on the flat Au(111), e.g., on the Au(211)  $d_{\text{O–Au}}$  is 2.051 Å. On Au(211), the O coverage is 1/6 ML and it is 1/8 ML on Au(221) because of their different terrace lengths. The increase of  $E_{\text{ad}}(\text{O})$  indicates that Au atoms on steps are more active and can bond with the O atom more strongly. It should be emphasized that the O atom chemisorption energy of 3.09 eV on Au(211) is still 1 eV lower than that on Pt(111) (4~4.3 eV),<sup>44</sup> where the  $\text{O}_2$  dissociative adsorption is observed experimentally.<sup>52–54</sup>

**Table 2.**  $\text{O}_2$  Dissociation Barriers,  $E_{\text{a}}(\text{O}_2\text{-dis})$ , and the TS Structures on Different Au Surfaces (O1 and O2 are Two Oxygen Atoms, which are Labeled in Figure 2)<sup>a</sup>

	$d_{(\text{O1–Au})}$ (Å)	$d_{(\text{O2–Au})}$ (Å)	$d_{(\text{O1–O2})}$ (Å)	$E_{\text{a}}(\text{O}_2\text{-dis})$ (eV)
Au(111)	2.145,2.308,2.370	2.176,2.209	1.932	2.23
Au(221)	2.290,2.265,2.239	2.133,2.140	1.919	1.16
Au(211)	2.198,2.234,2.351	2.130,2.113	1.910	0.93
Au kink-I	2.238,2.252,2.261	2.120,2.120	1.889	1.14
Au kink-II	2.205,2.312,2.383	2.176,2.198	1.901	1.28
29-atom	2.304,2.314,2.374	2.137,2.132	1.741	1.50

<sup>a</sup> In the TS structure, one O atom is on the 3-fold hollow site and the other O atom is on the bridge site. The  $d_{(\text{O1–Au})}$  are the O–Au bond distances between the O on the hollow and the three Au atoms, and the  $d_{(\text{O2–Au})}$  are the O–Au distances between the O atom on the bridge site and the two Au atoms.

**Figure 2.** Structures for the calculated TSs of  $\text{O}_2$  dissociation on Au(111) (a) and Au(211) (b). Small white balls represent the O atom, and the large white balls represent Au atoms on the step-edge atoms of Au(211). In (b), the O1 is close the fcc hollow site on the terrace.

Interestingly, on kinked Au surfaces the  $E_{\text{ad}}(\text{O})$  are only 2.72 and 2.71 eV for Au kink-I and kink-II, respectively. The adsorption site of O atom is the 2-fold bridge site (labeled as KB, Figure 1c and d). The CN of Au atoms bonded with the O atom at the kinks is 6 for both kink-I and kink-II and is smaller than those at the steps. This is quite surprising, because it has been long believed that the less coordinated the metal atoms, the more reactive they are. It appears that the decrease of the CN of Au atoms here plays a negative role for the O adsorption. We have also calculated the  $E_{\text{ad}}(\text{O})$  for an O atom on a Au adatom (a Au atom sitting on the fcc hollow site of Au(111) in a  $p(2 \times 2)$  unit cell). In this case, the Au CN is further reduced to 3 with the  $E_{\text{ad}}(\text{O})$  being only 1.73 eV (Table 1).

For small Au clusters that may be considered as models for Au particles, we found that the O atom chemisorption energies are quite low. The  $E_{\text{ad}}(\text{O})$  on the edge of the 12-atom cluster (EB site, shown in Figure 1e) is 2.58 eV, and it is 2.62 eV on a step-edge of the 29-atom cluster (EB site, shown in Figure 1f).

**3.1.2  $\text{O}_2$  Dissociation.** Having studied the O atom adsorption behavior, we then investigated the  $\text{O}_2$  dissociation on the Au surfaces. The calculated  $\text{O}_2$  dissociation barriers ( $E_{\text{a}}(\text{O}_2\text{-dis})$ ) on the different surfaces are listed in Table 2, together with the important structural parameters for all the TSs. For  $\text{O}_2$  dissociation on the flat Au(111), the transition state (TS) we located is similar to previous ones found for diatomic molecules, e.g., CO,  $\text{N}_2$ , NO dissociation on close packed transition metal surfaces:<sup>45,50</sup> One O atom is near the 3-fold fcc hollow site, and the other is near a bridge site. At such a TS, two O atoms bond with surface atoms tightly with short distances, and the bond length between the two O atoms is very long (Figure 2a). The TS belongs to a *late TS* because the TS is quite close to the

(52) Yoshinubo, J.; Kawai, M. *J. Chem. Phys.* **1995**, *103*, 3220.(53) Alleers, K.-H.; Pfnur, H.; Feulner, P.; Menzel, D. *J. Chem. Phys.* **1994**, *100*, 3985.(54) Eichler, A.; Hafner, J. *Surf. Sci.* **1999**, *58*, 433.

final state (FS). The calculated reaction barrier for the O<sub>2</sub> dissociation ( $E_a(\text{O}_2\text{-dis})$ ) on the flat Au(111) is very high (2.23 eV). This indicates that the O<sub>2</sub> dissociation on Au single crystals is impossible at low temperature, which is consistent with experimental findings.

On Au steps, kinks and the 29-atom cluster, the TSs for O<sub>2</sub> dissociation have a similar structure, which is, however, quite different from that on the flat Au(111). Figure 2b shows the TS structure of O<sub>2</sub> dissociation on the step of Au(211), which is the common structure for the O<sub>2</sub> dissociation on all the defects. At such a TS, the two O atoms sit on different layers of monatomic steps, and importantly no surface Au atoms are shared between the two O atoms. Consequently, the  $E_a(\text{O}_2\text{-dis})$  are largely reduced on these defects, compared to the  $E_a(\text{O}_2\text{-dis})$  on the flat Au(111) (2.23 eV). At the steps of Au(211), the  $E_a(\text{O}_2\text{-dis})$  is the lowest (0.93 eV); at the kinks the  $E_a(\text{O}_2\text{-dis})$  are slightly higher, about 1.1–1.3 eV; at the 29-atom cluster, the  $E_a(\text{O}_2\text{-dis})$  is even higher (1.50 eV). This order of reactivity, i.e., steps > kinks > cluster, is identical to that of  $E_{ad}(\text{O})$  (Table 1). It should be mentioned that we have also tested O<sub>2</sub> dissociation on many other Au different clusters with a size ranging from 12-atom (diameter < 1 nm) to 48-atom (diameter 1–2 nm), and all the  $E_a(\text{O}_2\text{-dis})$  were calculated to be more than 1 eV.

Having obtained the O<sub>2</sub> dissociation barriers, we are now in a position to address whether O<sub>2</sub> can dissociate on Au. First, the O<sub>2</sub> dissociation, if it occurs, should be only on Au steps because the  $E_a(\text{O}_2\text{-dis})$  on the steps are significantly lower than that on the flat surface. We rule out the possibility of O<sub>2</sub> dissociation on Au(111) owing to its enormous barrier (2.23 eV). Using the Arrhenius equation,  $s_0 \sim A \times \exp(-E_a/RT)$  ( $T = 300$  K,  $E_a = 0.93$  eV), to estimate the initial sticking coefficient ( $s_0$ ) of O<sub>2</sub> on Au steps, we obtain the  $s_0 \sim A \times 2.6 \times 10^{-16}$ . Further, if we take the value of  $A = 10^{-5}$  which was experimentally measured for N<sub>2</sub> dissociation on Ru(0001) (N<sub>2</sub> dissociation on Ru surfaces is found dominantly on Ru steps, see the paper by Dahl et al.<sup>46,47</sup>), it results in  $s_0 \sim 10^{-21}$ . This value is obviously very small, indicating that O<sub>2</sub> will not dissociate on unsupported Au.

**3.1.3 Physical Origin of O–Au Bonding and its Relation to O<sub>2</sub> Dissociation.** The adsorbate–metal bonding has been extensively studied for decades.<sup>49</sup> On the basis of the Anderson–Newns model,<sup>49a</sup> Hammer and Norskov<sup>49b</sup> suggested that the adsorbate–metal bonding is achieved via two steps: First, the charge transfer from the metal  $s/p$  orbitals to the adsorbate, leading to a broadening of the adsorbate valence states. Second, the broadened adsorbate valence states further mix with the localized metal  $d$  states. Consistent with this, one of our recent papers<sup>35</sup> addressed the O bonding on a Rh(111) surface. We showed clearly that the O atom bonding on transition metal surface possesses both ionic and covalent bonding characters.

To provide insight into the O–Au bonding, we first plotted the density of states projected on the  $d$  orbitals of Au atoms ( $d$ -PDOS) on the flat Au(111) (CN = 9), Au(211) (CN = 7) and Au kink-II (CN = 6) (before O atom adsorption). The plots are shown in Figure 3. As expected, it illustrates that the  $d$  bands of Au shift up toward the Fermi level as the CN decreases. The  $d$  band position has been widely used as a reactivity measure for metals by many workers,<sup>49,50</sup> in particular, by Hammer and

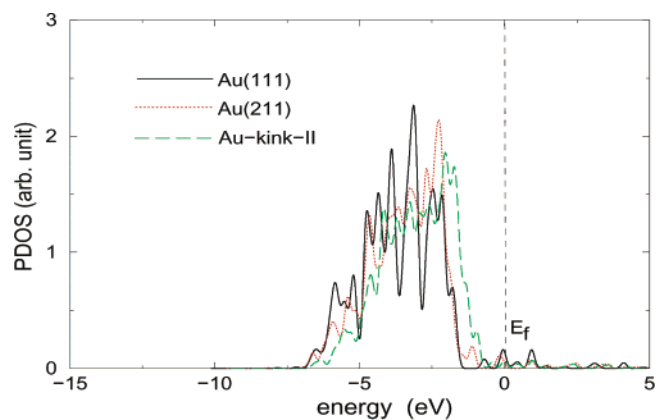


**Figure 3.**  $d$ -Projected density of states (PDOS) of the Au atoms in Au(111), Au(211) and Au kink-II. The Au atoms projected are those that will bond with O atoms. The Fermi level ( $E_f$ ) has been set to be zero.

**Table 3.** Mulliken Charge Analysis of Au Atoms in Au(111), Au(211), and Au Kink-II<sup>a</sup>

	$s/p$	$d$	total	net charge	CN
Au(111)	1.38	9.70	11.08	−0.08	9
Au(211)	1.29	9.73	11.02	−0.02	7
Au kink-II	1.21	9.75	10.96	+0.04	6

<sup>a</sup> The Au atoms calculated are the surface atom of Au(111), the step edge atom of Au(211) (shown in Figure 1b) and kink edge atom in Au kink-II (shown in Figure 1d). The coordination number (CN) of the Au atoms is also listed.

Norskov:<sup>49a</sup> The higher the  $d$  band center, the higher the reactivity. However, this model cannot explain the O–Au bonding: As the  $d$  band center shifts up, the O–Au adsorption strength first increases and then decreases.

To explain the oscillatory behavior of O–Au bonding on different surfaces, we then performed a Mulliken charge analysis on the same Au atoms. The Mulliken charges are obtained by projecting the total charge onto the  $s/p$  and the  $d$  atomic orbitals of the individual Au atoms. Mulliken analysis provides a useful indication of trends in changes in population of charge around atoms. The values are listed in Table 3. From the Mulliken charges, one can semiquantitatively compare the local electronic population of the atoms with respect to their atomic configuration, e.g., Au:  $5d^{10}6s^1$ . As shown in Table 3, the Au atom becomes more positively charged as it becomes less coordinated from Au(111) to Au kinks. We also notice that the electron depletion in the Au is mainly in the  $s/p$  orbitals (Table 3).

With the results above, the O–Au bonding with respect to the CN, namely the O–Au bonding increases from the CN of 9 to 7 and then decreases from the CN of 7 to 6, can be understood as follows. When an O atom sits on an Au surface, the energy gain with respect to the O atom and the Au surface separately, i.e., the O–Au bonding energy, can be divided into two components. The first component is the energy gain due to the charge transfer from the Au atoms to the O atom (the ionic component): In the isolated O atom, the electronic configuration is  $2s^2, 2p^4$ . Once the O atom is bonded with the Au surface, the electrons in the higher energy orbitals of Au, in particular, near the Fermi level, will move to the O empty  $p$  orbitals to lower their energies. The second component is the covalent contribution which is mainly the mixing between the O  $p$  orbitals and the Au  $d$  states (the energy of the O  $s$  orbital is too low to mix significantly with the Au  $d$  orbital). The covalent component,

$E_{\text{cov}}$ , can be estimated from the extended Huckel approximation<sup>49b,c,d</sup>

$$E_{\{\text{cov}\}} \sim - (1-f) \frac{V^2}{\epsilon_d - \epsilon_p} \quad (1)$$

where  $f$  is the metal  $d$  band filling;  $\epsilon_d$  and  $\epsilon_p$  are the band centers of metal  $d$  states and the O  $2p$  states, respectively;  $V$  is the coupling matrix element between the metal  $d$ -states and O  $2p$  states. Due to the Au  $d$  band being nearly fully occupied ( $1-f \sim 0$ ), the  $E_{\text{cov}}$  is very small (less than 0.1 eV) and thus not important. Therefore, the O–Au metal bond is largely determined by the ionic bonding. This may be the reason for why the  $d$  band center alone cannot explain the oscillatory behavior of O–Au bonding as a function of the CN.

The ionic bonding is determined by the population of high-energy electrons near the Fermi level of Au, which are predominantly of  $s/p$  character, with some  $d$  character. From Table 3, we can see that the population of Au  $s/p$  character states shrinks as the CN of Au decreases. This means that the Au  $s/p$  contribution to O–Au bonding decreases. On the other hand, the Au  $d$  band center shifts up, and thus, more high-energy  $d$  electrons become available as the CN of Au is reduced from 9 to 6. These competing contributions from the Au  $s/p$  states and the Au  $d$  states may be the answer to the oscillatory behavior of O–Au bonding as a function of the CN. This understanding may have some implications on the O chemisorption on small Au clusters: As the cluster size is reduced, the metallic character decreases which can be approximately measured by the decrease of the population of free electrons (mainly  $s/p$  states). As a result, the  $E_{\text{ad}}(\text{O})$  on small clusters is not high (see Table 1).

For O<sub>2</sub> dissociation, we found that the barrier,  $E_a(\text{O}_2\text{-dis})$ , spans more than 1 eV on different Au surfaces (Table 2). The O<sub>2</sub> dissociation on Au(211) possesses the lowest barrier, 0.93 eV. Naturally, an interesting question arises: why is there such a large difference in reactivity? An answer to this question can be found by considering the following two general factors.<sup>36,46,51</sup> (i) Geometrical factor. Recent experiments have shown that N<sub>2</sub> and NO dissociation on Ru are totally dominated by monatomic steps.<sup>46–48</sup> The enhanced activity at steps is attributed to a more favored *TS geometry* where no surface atoms are shared by the dissociating molecule. This can be applied in O<sub>2</sub> dissociation on Au. On the steps the two O atoms at the TS do not share bonding with surface atoms, whereas on Au(111) the two O atoms share bonding with one Au atom. The so-called bonding competition effect<sup>44,36,41,51</sup> will induce a large repulsive interaction between the two O atoms at the TS and, thus, increase the barrier. (ii) Electronic factor. It is known that the surface structure change will normally lead to the variation of the local electronic structure. This will in turn change the adsorption behavior of adsorbates, which finally affects the stability of TS of molecule dissociation on these surfaces. Our recent paper on CO dissociation<sup>36</sup> has shown that the CO dissociation barrier changes almost linearly as a function of the total chemisorption energy in the FS (the C chemisorption energy + the O chemisorption energy). Similar trends have also been observed in NO and N<sub>2</sub> dissociation by Hammer and Norskov.<sup>49b</sup> Therefore, it is reasonable that as the  $E_{\text{ad}}(\text{O})$  increases (the FS becomes more stable), the  $E_a(\text{O}_2\text{-dis})$  reduces. The electronic factor thus explains why O<sub>2</sub> dissociation is easiest on Au(211) (the  $E_{\text{ad}}(\text{O})$  on Au(211) is the highest).

**Table 4.** CO Adsorption Energy ( $E_{\text{ad}}(\text{CO})$ ) and the Adsorption Structures (the average C–Au Distance ( $d_{\text{C–Au}}$ ) and C–O Distance ( $d_{\text{C–O}}$ )) on Different Au Surfaces<sup>a</sup>

	Au(111)	Au(211)	Au(221)	12-atom cluster	Au-adatom
site	fcc	SB	SB	EB	top
$d_{\text{C–Au}}$ (Å)	2.205	2.109 <sup>(1/9 ML)</sup>	2.086 <sup>(1/12 ML)</sup>	2.040	1.983
$d_{\text{C–O}}$ (Å)	1.180	1.172 <sup>(1/9 ML)</sup>	1.173 <sup>(1/12 ML)</sup>	1.171	1.152
$E_{\text{ad}}(\text{CO})$ (eV)	0.17	1.05 <sup>(1/6 ML)</sup>	1.00 <sup>(1/8 ML)</sup>	1.25	1.03
		1.40 <sup>(1/9 ML)</sup>	1.31 <sup>(1/12 ML)</sup>		

<sup>a</sup> The  $E_{\text{ad}}(\text{CO})$  on Au-steps with different overages are also listed. The labelings of the CO adsorption site for Au(211), Au(221) are shown in Figure 1a and b.

**3.2 CO Adsorption and CO Oxidation.** As one would expect, there are two possible routes for CO oxidation on metal surfaces (i) CO+O→CO<sub>2</sub>; and (ii) CO+O<sub>2</sub>→CO<sub>2</sub>+O. In the first route, the O atom is a reactant, and thus, the O<sub>2</sub> dissociation is necessary before the CO oxidation. In the second route, an O<sub>2</sub> reacts directly with a CO. The adsorption of CO on the catalysts is essential in both routes. For CO adsorption on Au-based catalysts, many experimental works showed that CO can adsorb on small Au particles, but not on massive gold. In this subsection, we will show our calculated results for CO adsorption on Au surfaces and the CO oxidation via the above two routes.

**3.2.1 CO Adsorption.** Similar to atomic O chemisorption, we have investigated CO adsorption on several Au surfaces, i.e., Au(111), Au(211), Au(221), Au-adatom, and a 12-atom cluster (Figure 1e). The calculated  $E_{\text{ad}}(\text{CO})$  for CO adsorption energies and the important adsorption structures are listed in Table 4. It shows clearly that the CO can only weakly adsorb on the flat Au(111) ( $E_{\text{ad}}(\text{CO}) = 0.17$  eV). On surface defects, say steps, adatoms and clusters, the  $E_{\text{ad}}(\text{CO})$  is considerably increased, up to more than 1 eV. On Au-steps (Figure 1a and b), the most stable site for CO adsorption is the SB site, and the similar site, the EB site, on the 12-atom cluster (Figure 1e) was also investigated. These results suggest that CO can well adsorb on Au defects at the room temperature, which agrees with experiments. Considering that smaller Au particles will contain more defects (e.g., edges), we expect that the population of CO is sensitive to the size of Au particles. It is interesting to notice that the  $E_{\text{ad}}(\text{CO})$  is also sensitive to the CO coverage. For instance, on Au(221) the CO chemisorption energy at the coverage of 1/8 ML is 1.00 eV, which is about 0.30 eV lower than that at 1/12 ML.

From the results presented here and section 3.1, we can conclude that monatomic Au steps, e.g., the steps on Au(211) and Au(221), are the best sites for both CO and atomic O adsorption among all the sites. Moreover, these monatomic steps are quite common and easily available in real catalysts. Thus, we selected these steps as reaction sites to explore CO oxidation via the two possible routes: (i) CO+O→CO<sub>2</sub>; and (ii) CO+O<sub>2</sub>→CO<sub>2</sub>+O.

**3.2.2 CO + O → CO<sub>2</sub>.** We performed DFT calculations for CO + O → CO<sub>2</sub> near the step edge on both Au(211) and Au(221) surfaces. The most stable adsorption states of CO and O on each step (both CO and O are the most stable on the bridge site of steps), as listed in Table 1 and Table 4, are taken as the initial states. Then, we located the most stable TSs on both surfaces. The  $E_a$  is calculated according to eq 2

$$E_a = E_{\text{ad}}^{\text{IS}} - E_{\text{ad}}^{\text{TS}} \quad (2)$$

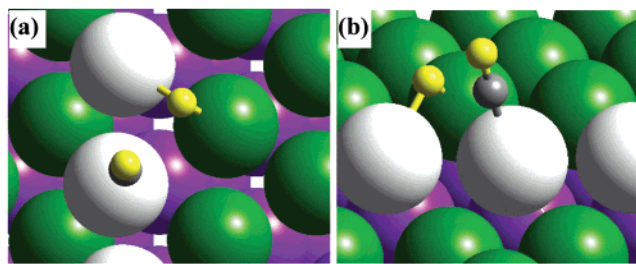


**Figure 4.** Structures of the calculated TS of the CO + O in which the O is an adsorbed O atom ( $O_a$ ) on Au(221). (a) and (b) are the top and side view of the TS, respectively. The C atom, O atom, step-edge Au atom, other terrace Au atom are represented by small gray balls, small white balls, large white balls, and large green balls, respectively. The important structural parameters are described as follows:  $d_{(O_a-Au_{edge})}$ : 2.126 Å;  $d_{(O_a-Au_{nonedge})}$ : 2.110 Å ( $Au_{nonedge}$  is the Au atom bonding with the  $O_a$ , but not at the edge);  $d_{(C-Au)}$ : 2.001 Å;  $d_{(C-O)}$ : 1.150 Å;  $d_{(C-O_a)}$ : 2.360 Å; Angle:  $\angle O-C-O_a$ : 106.0°

where  $E_{ad}^{TS}$  is the total chemisorption energy of CO and O at the TS:  $E_{ad}^{TS} = (E_{sur} + E_{CO} + E_O) - E^{TS}$ , in which  $E_{sur}$ ,  $E_{CO}$ ,  $E_O$ ,  $E^{TS}$  are the total energies of a clean surface, the CO molecule, the O atom and the TS (CO + O coadsorption at the TS structure), respectively; and  $E_{ad}^{IS} = E_{ad}(CO) + E_{ad}(O)$  (see Tables 1 and 4). On Au(221) the  $E_a$  is only 0.25 eV, whereas it is 0.68 eV on Au(211).

Because the reaction pathways for CO+O on the two steps are very similar, here we only discuss the one on Au(221). Initially, the O and the CO individually adsorb on the step-edge bridge sites. At the TS, the CO moves to an off-top site of the step-edge atom, whereas the O atom goes to a bridge site near the step, which is shown in Figure 4 (the important structure parameters for the TS are described in the figure caption). After the TS, a  $CO_2$  molecule is formed, which then desorbs from the Au surface. It is worth mentioning that the located TS, although near the step edge, is consistent with the general TS structure for CO + O reaction on close-packed transition metal surfaces.<sup>38–40,44,54</sup> Namely, the O atom must be activated to a bridge site to react with CO. Zhang and Hu<sup>39,40</sup> have rationalized this feature based on an electronic structure analysis. They found that the O atom  $2p$  orbitals are largely saturated in the IS, and thus have to be activated (the O atom is pushed to a bridge site) in order to enable the O to form new bond with the coming CO.

**3.2.3 CO + O<sub>2</sub> → OOCO → CO<sub>2</sub> + O.** In addition to the CO + O reaction pathway, we also located another low energy reaction pathway on Au steps, which involves the molecular O<sub>2</sub> as an initial reactant. This CO + O<sub>2</sub> reaction pathway features a meta-stable four-center O–O–CO intermediate state. Again the CO + O<sub>2</sub> reactions on the steps of Au(211) and Au(221) are very similar, and we only discuss the reaction on Au(221), which possesses a lower reaction barrier. In Figure 5, we show the important states along this pathway, namely TS1 (Figure 5a), a meta-stable intermediate (MS, Figure 5b) and TS2 (Figure 5c). The important structure parameters for these states are listed in Table 5. At the IS, the CO adsorbs on the step-edge bridge site of Au(221) and the O<sub>2</sub> is in the gas phase (we did locate a O<sub>2</sub> molecular adsorption state on Au(221), but the O<sub>2</sub> adsorption energy is too low (<0.05 eV) to be considered). Then, the O<sub>2</sub> approaches the CO, forming a four-center TS (TS1, Figure 5a). Over TS1, a meta-stable intermediate, the O–O–CO complex, is formed at the step edge (MS, Figure 5b). Then the O–O

**Table 5.** Structural Parameters for the Calculated States, Shown in Figure 5, for the CO + O<sub>2</sub> → CO<sub>2</sub> + O Reaction on Au(221)<sup>a</sup>

	$d_{(C-O)}$	$d_{(C-Au)}$	$d_{(C-O1)}$	$d_{(O1-O2)}$	$d_{(O2-Au)}$	$\angle_{(O-C-O1)}$
TS1	1.148	1.993	2.660	1.280	2.180	90.5
MS	1.203	2.091	1.358	1.421	2.113	118.9
TS2	1.200	2.130	1.276	1.741	2.122	130.6

<sup>a</sup> The unit of bond distance is Å and the unit of the angle is degree (°). TS1, MS, and TS2 are shown in Figure 5 and discussed in the text.

bond in the O–O–CO complex is stretch and the second TS (TS2, Figure 5c) is reached when the O–O bond is 1.74 Å. After TS2, a  $CO_2$  molecule is formed and an adsorbed O atom is left at the step edge. The adsorbed O atom can be easily removed by another CO, considering that the CO + O reaction can occur with only a 0.25 eV barrier, as shown before. It should be emphasized that the meta-stable intermediate state is not symmetrical (not a carbonate-like): the two O atoms of O<sub>2</sub> are chemically different with respect to the CO (Figure 5b).

In Figure 6 we show the total energy diagram of CO + O<sub>2</sub> reaction on the two Au steps. On Au(221) this pathway possesses a 0.59 eV barrier, and on Au(211) the barrier is 0.65 eV. Considering that under real CO oxidation conditions the CO coverage may be higher than we reported above (CO coverage = 1/12ML on Au(221)), which may affect the reaction barriers, we have also checked the CO coverage effect on the CO + O<sub>2</sub> reaction. We recalculated the CO + O<sub>2</sub> reaction using a (1 × 4) unit cell with two CO preadsorbed on the step bridge site of Au(221) (CO coverage = 1/8ML). In this unit cell, one CO reacts with the coming O<sub>2</sub>, and another CO is intact. The calculated  $E_a$  of the CO + O<sub>2</sub> reaction is reduced by 0.13 eV ( $E_a = 0.46$  eV), compared to the CO coverage of 1/12 ML. This indicates that the CO coverage effect is quite significant on the CO + O<sub>2</sub> reaction.

**3.2.4 Comparison of CO Oxidation on Different Metal Surfaces.** It is of interest to compare CO oxidation on Au to that on other metal surfaces. The CO + O<sub>2</sub> reaction on Pt(111) was calculated by Eichler and Hafner<sup>54</sup> using DFT. They found that CO can react with O<sub>2</sub> on Pt(111) with a small barrier (0.46 eV). The CO + O<sub>2</sub> reaction on Pt(111) was suggested to occur at low temperatures, i.e., 125–160 K. With a careful comparison, we found that the CO+O<sub>2</sub> on Au-steps are quite different from that on Pt(111), although their reaction barriers are almost the same (~0.46 eV): Molecular O<sub>2</sub> can adsorb on Pt(111) and can dissociate at nearly 200 K, whereas it cannot on Au, even at Au-steps. On Au-steps, the CO + O<sub>2</sub> reaction occurs through a unique O–O–CO intermediate state. On Pt(111), a  $CO_2$  forms through the O–O bond breaking and simultaneously the O–CO bond forming. Further comparing Au with Pt, we found that the CO + O reaction on Au-steps ( $E_a = 0.25$  eV) is much easier than that on Pt(111) ( $E_a = 0.76\sim 0.80$  eV).<sup>38,54,44</sup> In fact, the CO + O reaction on Au-steps is the easiest one among all the CO oxidation reported on different surfaces: on Ru(0001)  $E_a = 1.45$  eV,<sup>38,39,55</sup> on Rh(111)  $E_a = 0.91$  eV,<sup>38</sup> on Pt(111)  $E_a = 0.76\sim 0.80$  eV;<sup>38</sup> and on Ru-oxide (CO reacting with the bridging O on RuO<sub>2</sub>(110))  $E_a = 1.15$  eV.<sup>37</sup> In our previous paper,<sup>38</sup> we have shown that for CO oxidation on transition metal surfaces, the  $E_a$  is almost a linear function of the total chemisorption of reactants on metals ( $E_{ad}(CO) + E_{ad}(O)$ ) in the IS: The larger the total chemisorption energy of reactants in

(55) Stampf, C.; Scheffler, M. *J. Vac. Sci. Technol. A* **1997**, *15*, 1635.

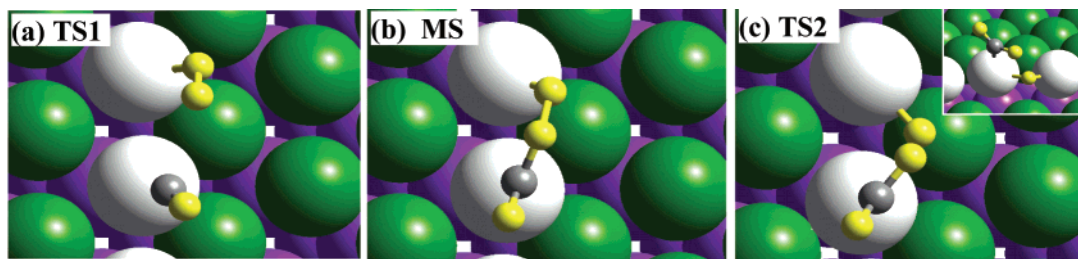


**Figure 5.** Structures of the calculated TS1 (a), meta-stable intermediate (MS) (b), and TS2 (c) of  $\text{CO} + \text{O}_2 \rightarrow \text{CO}_2 + \text{O}$  on Au(221) (also see Figure 6 for each state). The side view of the TS2 is also shown in the insert of (c). The C atom, O atom, step-edge Au atom, other terrace Au atom are represented by small gray ball, small white balls, large white balls, and large green balls, respectively. The important structural parameters of these states are listed in Table 5. The energetic diagram of the whole process is shown in Figure 6.

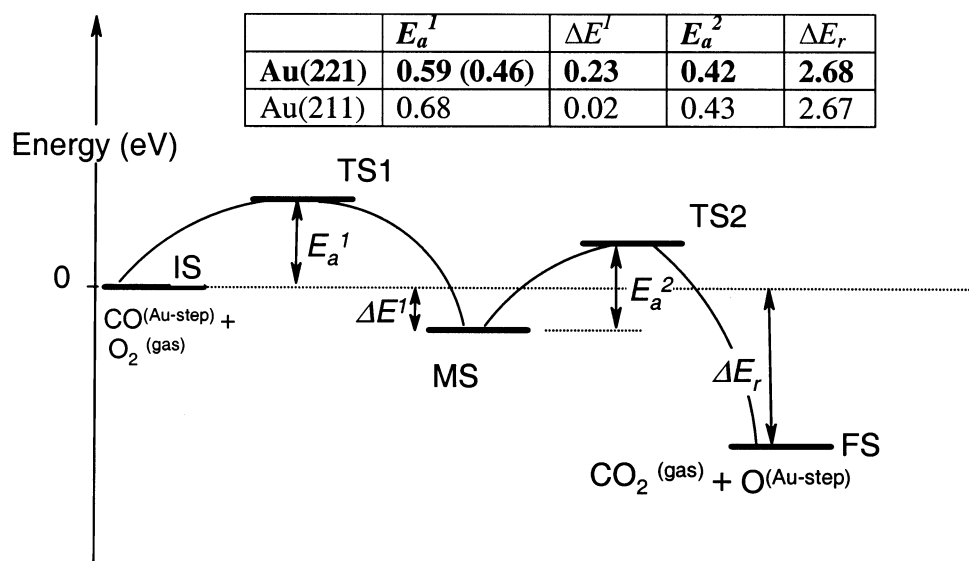


**Figure 6.** Schematic energetic diagram for  $\text{CO} + \text{O}_2 \rightarrow \text{CO}_2 + \text{O}$  reaction on Au(211) and Au(221), going through the IS, TS1, MS (meta-stable intermediate), TS2, and FS. On both surfaces, their ISs are taken as the energy zero. The values of the  $E_a^1$ ,  $E_a^2$ ,  $\Delta E^1$ , and  $\Delta E_r$  (labeled in the diagram) are listed in the inserted table, which corresponds to the CO coverage at 1/12 ML on Au(221) and 1/9 ML on Au(211). For the reaction on Au(221), we checked the CO coverage effect: when CO coverage increases from the 1/12 ML to 1/8 ML,  $E_a^1$  decreases from 0.59 to 0.46 eV, as listed in parentheses. All the energies are in eV.

the IS, the more difficult they are activated to have CO oxidation. The same reason can be applied to understand why the  $\text{CO} + \text{O}$  reaction on Au-steps is particularly easy. From our calculations, we obtained that the  $E_{\text{ad}}(\text{CO}) + E_{\text{ad}}(\text{O})$  on Au steps is 4.09 eV, about 2 eV lower than that on Pt(111), and more than 3 eV lower than that on Ru(0001).<sup>48,55</sup> Therefore, the high activity of Au is in fact due to its weak bonding ability with CO and O. It should also be noted that on the flat Au(111) the surface bonding ability is too low to “catch” CO molecule, and thus, no CO oxidation can occur, while the slightly more active sites, i.e., Au-steps, are the best sites for the  $\text{CO} + \text{O}$  reaction.

It should be emphasized that the reaction pathways of  $\text{CO} + \text{O}$  and  $\text{CO} + \text{O}_2$ , shown in Figures 4 and 5, respectively, possess a common feature: The reactions occur on the top layer edge of Au-steps without involving atoms on the terrace, which is very different from diatomic molecule dissociation, such as  $\text{N}_2$ ,  $\text{CO}$ , and  $\text{NO}$  on transition metal surfaces.<sup>48</sup> An important implication of this feature, we expect, is that any edges of Au particles can be potentially active for CO oxidation. The importance of the Au-edges (in Au particles) has been emphasized by Mavrikakis et al.<sup>22</sup> The CO oxidation on the edges of Au particles<sup>48</sup> is very similar to what we have presented in Figures 4 and 5.

**3.3 General Discussion of CO Oxidation on Au-Based Catalysts.** On the basis of our first principles calculations for CO oxidation on Au surfaces, we suggest the following: (i) CO oxidation can only occur on Au-steps. On Au single crystals where the step concentration is low, the CO oxidation rate must be low. (ii) CO oxidation may follow a bi-molecular  $\text{CO} + \text{O}_2$  reaction, through an O–OCO complex as an intermediate on Au-steps, which produces simultaneously a  $\text{CO}_2$  and an O atom on Au-steps, and the barrier is about 0.46 eV. (iii) CO can readily react with an O atom on Au steps. The barrier for this step is about 0.25 eV on Au-based catalysts.

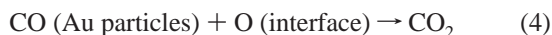
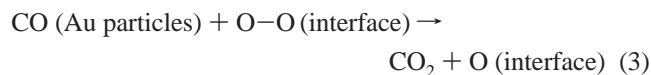
As mentioned in the Introduction, there are two types of supporting materials for Au-based catalysts: inert materials (irreducible oxide), such as  $\text{SiO}_2$  and  $\text{Al}_2\text{O}_3$  and active materials (reducible oxide), e.g.,  $\text{Fe}_2\text{O}_3$  and  $\text{TiO}_2$ . It is known that the inert materials play little role in chemical reactions apart from supporting dispersed metal particles in the catalytic systems of metal/inert-materials. Therefore, it is expected that the CO oxidation mechanism on Au/inert-materials will be similar to that on pure Au surfaces and particles. Hence, from our calculations for CO oxidation on Au clusters and Au surfaces, we suggest that CO oxidation on Au/inert-materials (such as  $\text{Al}_2\text{O}_3$ ) may start with a slow  $\text{CO} + \text{O}_2 \rightarrow \text{CO}_2 + \text{O}$  reaction, and then follow a fast  $\text{CO} + \text{O} \rightarrow \text{CO}_2$  reaction. Both reactions

only occur on *Au steps (edges)*, which means that the CO oxidation on Au catalysts is related to the population of steps. The CO + O<sub>2</sub> reaction should be the rate-determining step based on the following reasons: (i) the barrier of CO + O<sub>2</sub> is higher than the subsequent CO + O reaction; and (ii) the CO + O<sub>2</sub> reaction does not belong to a typical Langmuir–Hinshelwood mechanism because O<sub>2</sub> does not adsorb on Au well. This will significantly reduce the reaction possibility for CO + O<sub>2</sub> reaction.

Our calculation results are consistent with the experimental findings for CO oxidation on Au supported by inert materials: (i) It was observed in many experiments that the reaction rate of CO oxidation on Au-based catalysts is sensitive to the Au particle size.<sup>1,2,4,23</sup> As we expect, one of the reasons is that the concentration of Au steps, where CO can adsorb and CO oxidation can occur, may be related to the size of Au particles. (ii) CO oxidation on Au supported by inert materials is much slower than that on Au supported by active materials.<sup>23</sup> The reaction temperature of CO oxidation on Au/inert-materials is also much higher (above 323 K (50 °C), as observed by Grisel and Nieuwenhuys<sup>29</sup>) than that on Au/active-materials (can occur at a temperature as low as 200 K on Au/TiO<sub>2</sub>) (see the discussion below).

Two issues should be emphasized here: First, we rule out the possibility for O<sub>2</sub> direct dissociation on Au particles at low temperatures. However, O<sub>2</sub> dissociation is possible at elevated temperatures. Second, for CO oxidation on Au/inert-materials the particle size effect, which is related to the population of Au steps, is associated with the CO adsorption and the consequent CO oxidation reactions. This is different from the conventional view that O<sub>2</sub> dissociation is sensitive to the particle size.

It is of interest to extend our understanding of the mechanism of CO oxidation on Au/active-materials, such as Au/TiO<sub>2</sub>. As discussed above, the major problem for Au/inert-materials is that O<sub>2</sub> does not adsorb (too weakly chemisorbed) on Au particles, leading to the CO oxidation through the CO+O<sub>2</sub> reaction, which is intrinsically not fast. This problem may be overcome in Au/active-materials. Iwasawa et al.<sup>18,28</sup> have observed the O<sub>2</sub> adsorption on Au/Ti(OH)<sub>4</sub> and Au/TiO<sub>2</sub> in ESR experiments. Haruta et al.<sup>1,2</sup> suggested that O<sub>2</sub> may first adsorb on the Au-oxide interface, and then react with the CO on the Au, as described in the following



Haruta et al. further proposed a symmetrical –CO<sub>3</sub> carbonate-like intermediate for the CO + O<sub>2</sub> reaction.

To check this, we carried out a preliminary calculation for O<sub>2</sub> adsorption on the interface of Au/TiO<sub>2</sub>(110). In the calculation, TiO<sub>2</sub>(110) was modeled by 6 layers slab with a large unit cell of (2 × 2) (8.91 × 13.14 Å, in all 16 units of TiO<sub>2</sub> per slab)).<sup>56</sup> A 16-atom cluster of Au was placed in the center of the unit cell and O<sub>2</sub> was put on the Au/TiO<sub>2</sub> interface. After optimization, one O atom was found to bond with a top-layer Ti atom on the TiO<sub>2</sub>(110) and the other O atom was found to

bond with a Au atom at the Au-cluster edge. The chemisorption energy of the O<sub>2</sub> is about 0.8 eV, which is substantially greater than the  $E_{\text{ad}}(\text{O}_2)$  on pure Au. On the basis of our calculations, we would suggest the following: (i) The reaction of CO+O<sub>2</sub> on Au/active-materials follows a Langmuir–Hinshelwood mechanism because of the reasonable chemisorption energy of both CO and O<sub>2</sub>, which may considerably increase the reaction rate, compared to the same reaction on Au/inert materials. (ii) The symmetrical carbonate intermediate probably does not exist; it was not found on Au in our calculations. The most likely intermediate that could mimic the –CO<sub>3</sub> carbonate of Haruta et al. is shown in Figure 5b, in which one O atom of O<sub>2</sub> contacts with the CO, and the other O atom adsorbs on the active metal oxide. Experimentally, Schubert et al.<sup>23</sup> indeed demonstrated in an isotopic exchange experiment that CO oxidation on Au-based catalysts should not experience a symmetrical carbonate-like intermediate. (iii) The Au/metal-oxide interface plays important roles in the catalytic process, which is related to both the Au loading and the Au particle size. This has already been discussed in detail by Schubert et al.<sup>23</sup>

Finally, an interesting question arises: considering that the CO + O<sub>2</sub> reaction can also occur on Pt with a similar barrier as on Au, why do only Au-based catalysts show high reactivity? We believe that the following two problems exist on Pt. (i) O<sub>2</sub> can easily dissociate on Pt at very low temperature (also true for other transition metals). This reduces greatly the possibility of CO + O<sub>2</sub> on Pt; (ii) Once the O<sub>2</sub> dissociates, the CO oxidation through the CO + O reaction possesses intrinsically a high barrier on Pt compared to that on Au. In general, the inertness of Au provides the possibility of the CO + O<sub>2</sub> reaction and also largely facilitates the CO+O reaction.

#### 4. Conclusions

This work represents one of the first attempts to obtain a comprehensive picture of CO oxidation on Au surfaces using DFT calculations: Many possible elementary reactions in CO oxidation on a range of Au surfaces were calculated. A deeper understanding of the reaction mechanism of CO oxidation on Au-based catalysts has been obtained. The following conclusions are reached:

(i) The O atom chemisorption energy on Au surfaces follows the order: steps > kinks > flat Au(111). The maximum chemisorption energy is reached when the O is on the step. The O–Au bonding on small Au particles is similar to that on flat Au(111), not stronger than that on steps. The O–Au bonding nature is discussed with respect to the Au electronic structure.

(ii) The barriers of O<sub>2</sub> dissociation on Au surfaces are generally very high. The lowest barrier is 0.93 eV, which occurs on steps of Au. It is expected that O<sub>2</sub> cannot dissociate at low temperatures, but it may be possible on steps at elevated temperatures. The gold particle size does not play an important role in helping the O<sub>2</sub> dissociation.

(iii) CO can well adsorb on Au defects, but rather poorly on flat Au(111). This implies that CO adsorption is sensitive to the population of Au defects and thus to the gold particle size.

(iv) CO can readily react with atomic O with a very low barrier (0.25 eV on Au-steps).

(v) O<sub>2</sub> can directly react with CO on Au-steps with a low barrier, ~0.46 eV. This CO + O<sub>2</sub> route features an unsymmetrical four-center O–O–CO meta-stable intermediate on steps.

(56) Ramamoorthy, M.; D. Vanderbilt and King-Smith, R. D. *Phys. Rev. B* **1994**, *49*, 16 721.

(vi) CO oxidation on Au/inert materials may occur through the reaction of  $\text{CO} + \text{O}_2 \rightarrow \text{CO}_2 + \text{O}$  on Au steps (described in (v)) and followed by  $\text{CO} + \text{O} \rightarrow \text{CO}_2$ .

An additional calculation was carried out to investigate the  $\text{O}_2$  adsorption on the interface of Au/TiO<sub>2</sub>. It was found that  $\text{O}_2$  can adsorb at the interface of Au/TiO<sub>2</sub>(110) with a reasonable chemisorption energy ( $\sim 0.8$  eV). It is likely that CO oxidation on Au/active-materials follows the same mechanism as described in (vi) except that the  $\text{O}_2$  may chemisorb on the interface and

the reaction of  $\text{CO} + \text{O}_2 \rightarrow \text{CO}_2 + \text{O}$  follows a Langmuir–Hinshelwood mechanism. Further work of CO oxidation on Au/active-materials is being carried out.

**Acknowledgment.** We gratefully acknowledge the UKCP for computing time in T3E and the supercomputing center in Ireland for computing time in IBM-SP. Z.-P.L. thanks The Queen's University of Belfast for a studentship.

JA0205885